Metabolomics (2023) 19:83
https://doi.org/10.1007/s11306-023-02044-4

ORIGINAL ARTICLE

Impact of hypoxia and reoxygenation on the extra/intracellular metabolome and on transporter expression in a human kidney proximal tubular cell line

Quentin Faucher[1] · Stéphanie Chadet[2] · Antoine Humeau[1,5] · François-Ludovic Sauvage[1] · Hélène Arnion[1] · Philippe Gatault[2,3] · Matthias Buchler[2,3] · Sébastien Roger[2] · Roland Lawson[1] · Pierre Marquet[1,5] · Chantal Barin-Le Guellec[1,4]

Received: 4 October 2022 / Accepted: 21 August 2023 / Published online: 13 September 2023

Abstract

Introduction Ischemia-reperfusion injury (IRI) induces several perturbations that alter immediate kidney graft function after transplantation and may affect long-term graft outcomes. Given the IRI-dependent metabolic disturbances previously reported, we hypothesized that proximal transporters handling endo/exogenous substrates may be victims of such lesions.

Objectives This study aimed to determine the impact of hypoxia/reoxygenation on the human proximal transport system through two semi-targeted omics analyses.

Methods Human proximal tubular cells were cultured in hypoxia (6 or 24 h), each followed by 2, 24 or 48-h reoxygenation. We investigated the transcriptomic modulation of transporters. Using semi-targeted LC–MS/MS profiling, we characterized the extra/intracellular metabolome. Statistical modelling was used to identify significant metabolic variations.

Results The expression profile of transporters was impacted during hypoxia (y + LAT1 and OCTN2), reoxygenation (MRP2, PEPT1/2, rBAT, and OATP4C1), or in both conditions (P-gp and GLUT1). The P-gp and GLUT1 transcripts increased (FC (fold change) = 2.93 and 4.11, respectively) after 2-h reoxygenation preceded by 24-h hypoxia. We observed a downregulation (FC = 0.42) of y^+LAT1 after 24-h hypoxia, and of PEPT2 after 24-h hypoxia followed by 2-h reoxygenation (FC = 0.40). Metabolomics showed that hypoxia altered the energetic pathways. However, intracellular metabolic homeostasis and cellular exchanges were promptly restored after reoxygenation.

Conclusion This study provides insight into the transcriptomic response of the tubular transporters to hypoxia/reoxygenation. No correlation was found between the expression of transporters and the metabolic variations observed. Given the complexity of studying the global tubular transport systems, we propose that further studies focus on targeted transporters.

Keywords Proximal tubular cells · Ischemia-reperfusion injury · Membrane transporters · Metabolomics · Statistical modeling

✉ Pierre Marquet
pierre.marquet@unilim.fr

1 U1248 Pharmacology & Transplantation, INSERM and Univ. Limoges, 87000 Limoges, France

2 EA4245, Transplantation, Immunologie, Inflammation, Univ. Tours, 37000 Tours, France

3 Nephrology and Immunology Department, Bretonneau Hospital, 37000, Tours, France

4 Department of Biochemistry and Molecular Biology, CHRU de Tours, 37000, Tours, France

5 Department of Pharmacology, Toxicology and Pharmacovigilance, University Hospital of Limoges, 87000 Limoges, France

1 Introduction

Kidney transplantation is the gold standard treatment for patients with end-stage renal disease. Given the high prevalence of kidney diseases (WHO 2021), the gap between the needs and the number of organs donated for transplantation will continue to rise. Faced to this growing shortage, transplantation centers are broadening the criteria for organ acceptability by allowing the procurement of "sub-optimal" grafts, including from donors after cardiac death and extended criteria donors. However, kidneys from these donors are more prone to ischemia-reperfusion injury (IRI) (Wong et al. 2017 & Zhao et al.

2018), which is a frequent and serious complication in kidney transplantation, associated with delayed graft function in the post-implantation period. IRI is a complex, multifactorial and prolonged pathophysiological process, associated with numerous structural and metabolic disturbances. IRI induces the development of interstitial fibrosis and the amplification of the local immune response, which accelerates the loss of renal function and shortens graft survival (Zhao et al. 2018 & Chen et al. 2015). This requires improved understanding of the pathogenicity of these lesions. Metabolomic profiling analyses focusing on ischemia or ischemia-reperfusion (IR) in vivo have been performed (Malagrino et al. 2016 & Faucher et al. 2022). Numerous metabolites identified in perfusion solutions or bio-fluids were reported to be released from injured cells or related to the inflammatory response. Other metabolites may arise from tubular damage and/or impaired renal tubular function. Proximal tubular cells (PTC) are the most sensitive to IRI, especially since they spend a lot of energy for the transfer of substrates from blood to urine or vice versa. These trans-epithelial movements are governed mainly by the coordinated activity of tubular transporters of the SLCs (Solute Carriers) and ABCs (ATP-Binding Cassette) super-families (Faucher et al. 2020 & Barin-Le Guellec et al. 2018). Lesions associated with ischemia are accompanied by a functional alteration of tubular transporters. These alterations, observed in pre-clinical models of warm ischemia, persist during reperfusion and could influence graft outcomes (Faucher et al. 2020). Given the major role of transporters in renal and organism homeostasis, alterations in their activity could partially explain delayed recovery of graft function after transplantation, representing a risk of global metabolic disturbances, accumulation of toxins and overexposure to drugs in the immediate post-transplant period (Faucher et al. 2020 & Barin-Le Guellec et al. 2018). The aim of this exploratory study was to determine the impact of hypoxia and reoxygenation on the expression of tubular transporters and the intra- and extra-cellular metabolome composition in a human proximal tubular cell line.

2 Methods

2.1 Cell culture condition

RPTEC/TERT1 human proximal tubular cells (ATCC® CRL-4031™) were expanded in 175cm^2 flasks at 37 °C with 5% CO_2 in a serum-free hormonally-defined medium (RPTECm) consisting of a mixture of DMEM/F-12(1:1) (1X) + GlutaMAX™ (ThermoFisher; #31331-028), supplemented with a commercially hTERT Immortalized RPTEC Growth kit (ATCC® #ACS-4007), and 0.1 mg/mL G-418 (Sigma-Aldrich; #04727878001). Cells were subcultured after establishing a contact-inhibited monolayer and reseeded at 100% confluence density in plastic culture plates for further experiments. Cells were grown for at least 14 days to reach a differentiated state with medium replacement three times per week (Secker et al. 2019 & Aschauer et al. 2015). For Hypoxia (H) and Hypoxia/Reoxygenation (H/R) experiments, RPTEC/TERT1 differentiated cells were submitted to 6-h or 24-h hypoxia (1% O_2, 5% CO_2, RPTECm) in a hypoxia chamber (INVIVO2 200, Ruskinn Technology, AWEL international). RPTECm were equilibrated overnight in the hypoxia chamber before the experiment. Hypoxia incubations was followed or not by different periods of reoxygenation (21% O_2, 5% CO_2, RPTECm). For each H or H/R culture condition, a control with a similar normoxic (N) culture period (21% O_2, 5% CO_2, RPTECm) was performed, to account for the variations in culture timing and duration. For the normoxic controls of hypoxic conditions without reoxygenation, the medium was equilibrated overnight before the experimentation. The overall culture conditions are summarized in Figure S1. RPTEC/TERT1 cells were used at passages 20–30.

2.2 Transcriptional expression of tubular transporters

For each incubation condition, RNA was extracted using the Nucleospin RNA/Protein kit (740933.50, Macherey-Nagel), according to manufacturer instructions. RNA concentration was estimated using Qubit 4.0 with the Qubit™ RNA BR Assay Kit (Q10210, Invitrogen™). RNA quality was assessed by RNA Integrity Number (RIN) determination with Agilent RNA 6000 Pico kit and a Bioanalyzer 21 000 (Agilent). One-µg RNA samples from each duplicates were pooled and the concentration estimated. cDNA was synthesized from 1 µg RNA using the High-capacity cDNA Reverse Transcription kit (4,368,814, Applied Biosystems™), according to manufacturer instructions. Using custom-designed and manufactured TLDA cards we investigated the mRNA level of 40 genes coding mostly for tubular transporters and housekeeping genes chosen according to the literature (Wang et al. 2019). More detail on manufacturer instructions are provided as Supplementary Material, and the list of probe sets and manufacturer codes for TaqMan probes in Supplementary Table 1. The mRNA expression of tubular transporters was then analyzed using the comparative $2^{-\Delta\Delta Ct}$ method with NME4, CHFR, and C16orf62 as housekeeping genes. Two independent experiments were performed in duplicate. Only genes with a proper amplification curve were included in our analysis. Heat maps were built with the software MeV_4_9_0.

2.3 Metabolomic profiling

At the end of the incubation periods (H, H/R or N) the supernatants were collected to analyze the extracellular metabolome), the cells were lysed and the liquid phase collected to analyze the intracellular metabolome. The native medium was collected at each incubation time, as well as before and after overnight equilibration. For each independent experiment, a novel RPTECm was prepared. Three independent experiments were performed in triplicate.

2.4 Extraction of extracellular metabolites

Metabolite extraction was performed following the recommendations of the LC–MS/MS "Method Package for Cell Culture Profiling Ver.2" (Shimadzu), using 2-isopropylmalic acid as the internal standard. The supernatants collected were centrifuged at 3,000 rpm for 1 min at room temperature. A mixture of 100 µL supernatant, 200 µL acetonitrile, and 20 µL internal standard solution (2-isopropylmalic acid [0.5 mmol/L]), was prepared and strongly stirred. After centrifugation at room temperature for 15 min at 15,000 rpm, the supernatant was diluted 1/10 with ultrapure water (to avoid intensity saturation of some metabolites, ionization competition and to minimize matrix effects), and injected in the analytical system.

2.5 Extraction of intracellular metabolites

Intracellular metabolite extraction was adapted from a previously published method (Yuan et al. 2012). Briefly, cells were washed with ice-cold PBS and then lysed with 2 ml of 80% (vol/vol) methanol in ultrapure H_2O containing the internal standard (2-Isopropylmalic acid [0.5 mmol/L]) at 1/1000th, before incubation for 20 min at − 80 °C. Each well was scrapped, the cell lysate/methanol mixture were split and transferred into two distinct tubes to improve evaporation efficiency. Each tube was centrifuged at 11,000 *g* for 10 min at 4 °C to pellet cell debris. The metabolite-containing supernatant was transferred into a new tube and evaporated to dryness in a vacuum concentrator at room temperature. The extract was then solubilized with 55 µL of ultrapure H_2O. The content of the two tubes corresponding to the same sample/well was pooled. One hundred µL were transferred into vials for injection.

2.6 LC–MS/MS-metabolomic analysis

Mass spectrometry analysis was performed using a LCMS-8060 (Shimadzu) tandem mass spectrometer operated following the "Method Package for Cell Culture Profiling Ver.2" (Shimadzu). Chromatographic separation was carried out using a Discovery HS F5-3 column (150 × 2.1 mm d.i., 3 µm) and ionization was performed in the electrospray mode. The compounds were detected in the scheduled MRM (Multi Reaction Monitoring) mode in the positive and negative polarities alternately. One quantification and a minimum of one confirmation ion transitions, as well as the relative retention times were used for compound identification (Supplementary Table 2). For each transition analyzed, only well-defined chromatographic peaks were considered. Raw spectrometric data sets were normalized (area ratio (AR)) to the intensity of 2-isopropylmalic acid as internal standard. More details on mass spectrometry analysis are provided in Supplementary Methods and the complete list of metabolites screened is available in Supplementary Table 2.

2.7 Statistical analysis

In order to study the variations in the concentration of metabolites inherent to H and H/R we normalized the LC–MS/MS AR in hypoxia (reoxygenation) by the AR in normoxia. We could not divide by the mean value, because some metabolites were missing in normoxia. Thus, we divided by the sum of AR in normoxia and hypoxia resulting in the Normalized Area Ratio (NAR) (Figure S2).

Modeling was processed independently for the intracellular and extracellular media, using R 4.1.0 software and the brms 2.16.1 package. The outcome (the NAR in hypoxic condition) was modeled using a Gaussian family. The explanatory variables were hypoxia duration (oxie_t), reoxygenation duration (reox_t) and metabolites (metabolite). The model formula in brms was:

NAR ~ 0 + Intercept + oxie_t + mo(reox_t) + oxie_t:mo(reox_t) + (oxie_t:reox_t || metabolite), sigma ~ metabolite.

For more details on statistical analysis please refer to Supplementary Methods. The priors for each parameter are presented in Supplementary Table 3. The scripts used are available at https://inserm_pharmacology_limoges.gitlab.io/2023_faucher_sd_statistics_metabolomics/.

3 Results

3.1 Hypoxia-induced sublethal PTC condition

We did not observe significant evolution of LDH release, reflecting the cytotoxicity, over time in normoxia (Figure S3). We found no noticeable cytotoxicity after 6 h of hypoxia, alone or followed by 2, 24, or 48 h of reoxygenation. Actually, cytotoxicity reached a maximum of $6.3 \pm 0.6\%$ after 48 h of reoxygenation. No cytotoxicity was observed either after 24 h of hypoxia alone.

In contrast, we found a significant increase after 2 h (9.46 ± 1.39 vs. 3.96 ± 0.61; p = 0.0025), 24 h (14.14 ± 2.79 vs. 5.66 ± 0.35; p = 0.012) and 48-h (16.9 ± 3.02 vs. 8.23 ± 0.73; p = 0.0162) reoxygenation, as compared to normoxia. Figure 1 shows the metabolic signature of Krebs cycle intermediates (e.g., decreased of citric acid after 6 h (p = < 0.0001) and 24-h hypoxia (p = 0.0003) and anaerobic glycolysis (e.g., increased of lactic acid after 6 h (p = < 0.0001) and 24-h hypoxia (p = < 0.0001), relative to normoxia.

Intracellular metabolomic analysis in H vs. N conditions. The percentage of H compared to N (green dotted line) is represented by the blue aligned dot plot with mean ± s.e.m for metabolites of glycolysis and TCA cycle, **p < 0.01, ***p < 0.001, ****p < 0.0001 by unpaired t-test with Welch's correction. Comparison between H-incubated cells during 6 and 24 h, ##p < 0.01 and ###p < 0.001 respectively, was performed using unpaired t-test with Welch's correction. 6 and 24 h hypoxia conditions have their own independent N control (n = 3 independent experiments in triplicate). Statistical analysis was performed using the unpaired t test with or without Welch's correction as implemented in GraphPad Prism (v. 5.04). For more details on all statistical tests performed, please refer to Supplementary Table 4.

3.2 Expression of tubular transporters

H and H/R conditions did not induce RNA degradation, as shown by mean RIN values of 9.7 ± 0.01 (data not show). Among the targeted genes, we did not detect *slc22a6*, *slc22a7*, *slc22a8*, *slc22a11*, *slc2a2*, *slc5a1*, *slc47a2, slc47a1*, *slc22a2*, *slc13a2*, *slc22a12 and abcg2*. For the transporters detected, a heatmap representation shows the different expression patterns (fold-change (FC)) in the H and H/R conditions as compared to their respective N control (Fig. 2a). The fold-change values are summarized in Supplementary Table 5. Figure S4 shows the "physiological" variations of transcriptional expression in normoxic conditions. We have focused on consistent variations over time, since sporadic variations could be false positives.

We observed downregulation of all aquaporins after 24-h hypoxia (FC = 0.37 for AQP1, 0.06 for AQP2, and 0.42 for AQP3) (Fig. 2b), likely maintained up to 48 h of reoxygenation for AQP1 (FC = 0.54) and AQP2 (FC = 0.23) and up to 2 h for AQP3 (FC = 0.32). For AQP2 we observed a downregulation at 6-h hypoxia (FC = 0.54) followed by an upregulation after 24 h (FC = 2.20), further accentuated after 48-h reoxygenation (FC = 10.77). Regarding ABC transporters (Fig. 2c), the amount of transcripts coding for P-gp (abcb1) did not vary after 6-h hypoxia, whereas a decreasing trend was observed after 24 h (FC = 0.51) of hypoxia and up to 24-h reoxygenation

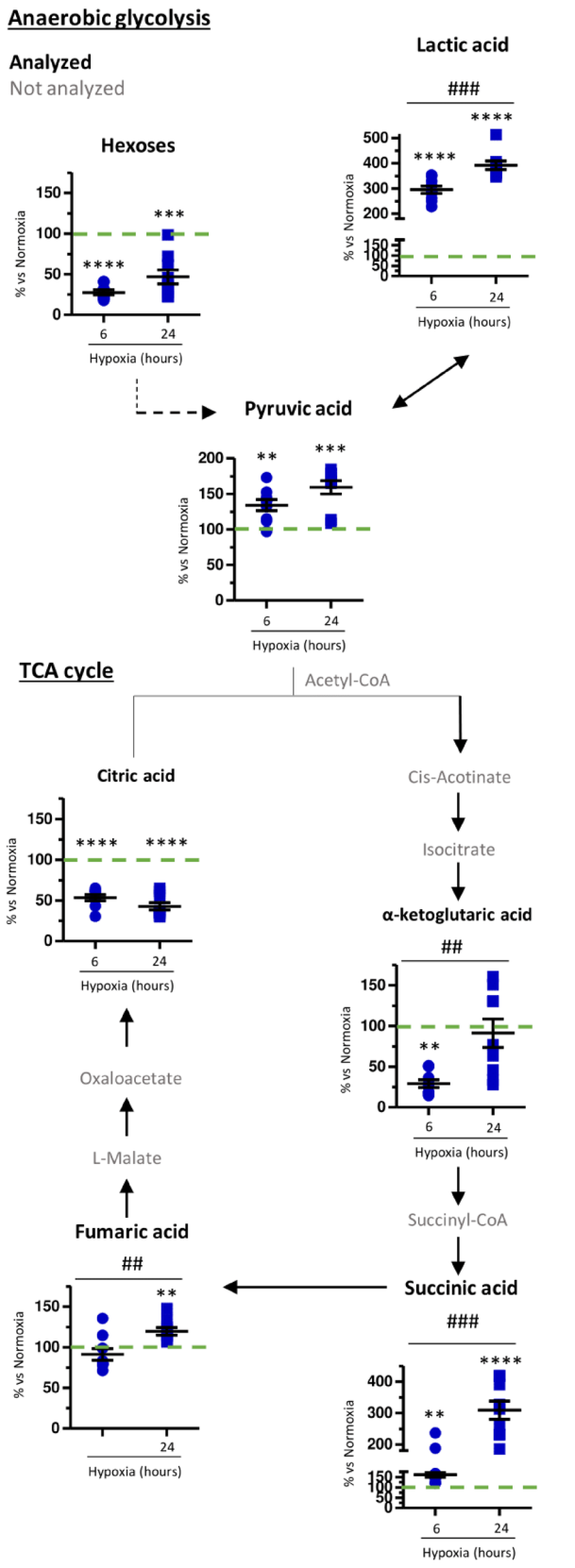

Fig. 1 Evolution of anaerobic glycolysis and TCA cycle intermediates under hypoxia

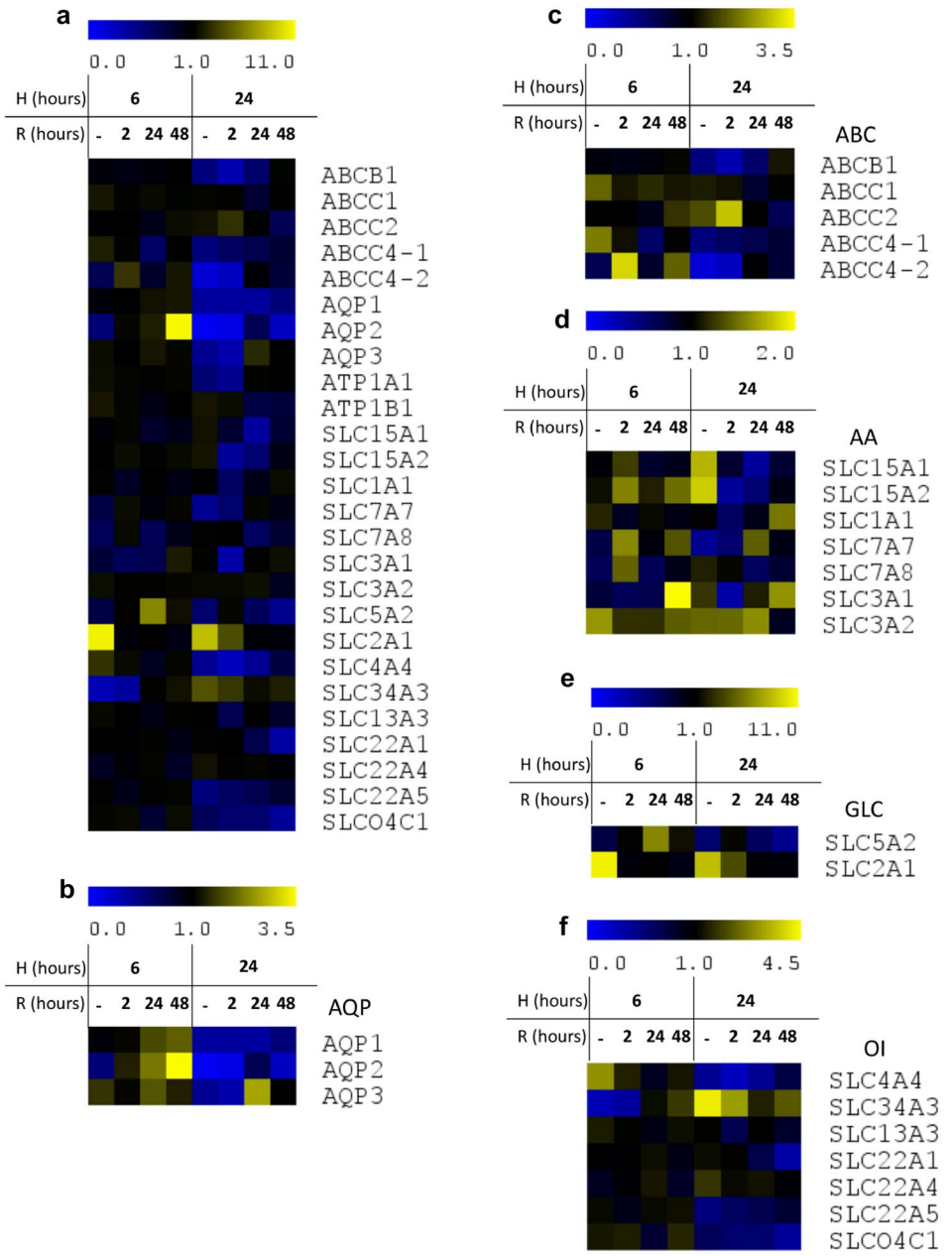

Fig. 2 Transcriptional expression of tubular transporters under H and H/R conditions

(FC = 0.30 after 2 h and 0.58 after 24 h). MRP2 (*abcc2*) mRNA increased (FC = 2.93) after 2-h reoxygenation preceded by 24-h hypoxia. For the amino acid transport system (Fig. 2d), we observed a downregulation (FC = 0.42) of y^+LAT1 (*slc7a7*) after 24-h hypoxia and of PEPT2 (*slc15a2*) and rBAT (*slc3a1*) after 2-h reoxygenation preceded by 24-h hypoxia (FC = 0.40 and 0.33, respectively). For the latter, we also observed an increase after 48-h reoxygenation preceded by 6-h hypoxia (FC = 2.08). We observed an increased quantity of transcripts encoding for GLUT1 (*slc2a1*) after 6 (FC = 10.56) and 24-h hypoxia (FC = 8.58), and even after 2-h reoxygenation (FC = 4.11) (Fig. 2e). There was a decreasing trend for OCTN2 (*slc22a5*) after 24 h of hypoxia (FC = 0.51) as well as a decrease for OATP4C1 (*slco4c1*) and OCT1 (*slc22a1*) after 48-h reoxygenation preceded by 24-h hypoxia (FC = 0.41 and 0.36, respectively) (Fig. 2f).

Heat map representation of TLDA results. Heat map shows the global gene fold-change expression pattern according to H and H/R conditions as compared to their own independent N control. Shades of yellow indicate upregulation, shades of blue downregulation and black unchanged expression. Color intensity reflects the fold-change value (n = 2 independent experiments in duplicate). Heat maps display (**a**) all detected transporters and (**b–f**) individual subgroups; (**b**) aquaporins, (**c**) ABC transporters, (**d**) amino

acids transporters, (**e**) glucose transporters, and (**f**) organic anions transporters. AA, amino acid; ABC, ATP-Binding Cassette; AQP, aquaporins; GLC, glucose; OI, organic ions.

3.3 Metabolomic profiling under H and H/R conditions

We documented the "physiological" variation kinetics of the PTC metabolome in normoxic conditions and the stability of the internal standard (2-Isopropylmalic acid). Results and data processing are summarized at https://inserm_pharmacology_limoges.gitlab.io/2023_faucher_sd_statistics_metabolomics/.

3.4 Intracellular metabolome

Intracellular metabolome profiling showed that the majority of metabolites are unaffected by hypoxia. However, some metabolites had increased after 6-h hypoxia, e.g. indole-3-acetic acid, lactic acid (Fig. 3a), or 24-h hypoxia, e.g. indole-3-acetic acid, choline (Fig. 3b), compared to their respective normoxic controls and the other metabolites. Others had decreased after 6-h hypoxia, e.g. thymine, adenosine (Fig. 3a), or 24-h hypoxia, e.g. cytidine monophosphate, deoxycytidine (Fig. 3b). Metabolites that increased or decreased upon 2, 24, or 48 h reoxygenation following 6 or 24-h hypoxia are summarized in Table 1 – Part 1. Some metabolites progressively increased with hypoxia duration e.g. citrulline, arginine, uridine, whereas others decreased e.g. pyridoxal phosphate, N-acetylaspartic acid, 2-aminoadipic acid. We also compared the metabolomic profiles during reoxygenation: after 2-h reoxygenation we found higher amounts of uridine, phenylalanine and tryptophan, in contrast to lower concentrations of deoxycytidine and glutathione. All metabolites returned to normal after 24-h reoxygenation excepted for hypoxanthine which was found in higher quantities after 48-h reoxygenation. Pathway analyses showed that the metabolites dysregulated after 6-h hypoxia belonged mainly to the metabolism of alanine, aspartate and glutamate on the one hand, and glutathione and purine on the other (Figure S5a). The metabolites dysregulated after 24-h reoxygenation are mainly involved in the phenylalanine, tyrosine and tryptophan biosynthesis pathway (Figure S5b). Besides, this pathway is the most discriminative between the 6- and 24-h hypoxia conditions (Figure S5c).

Posterior predictive distribution of metabolites in conditions of (**a**) 6-h and (**b**) 24-h hypoxia without reoxygenation, in the intracellular environment. The points represent the mean values, the thick and thin segments respectively the 80 and 98% confidence intervals of the posterior distribution. The green line (mean) and rectangles (80% and 98% confidence intervals) are the posterior predictive distribution irrespective of metabolite. Metabolites are in red (over abundant) or blue (under abundant) if their 98% confidence intervals do not cross the 98% confidence interval for all the metabolites.

3.5 Extracellular metabolome

We investigated the metabolomics profile of the native medium under N, H, and H/R to document any degradation or generation of metabolites. When compared to the results obtained on the extracellular medium, these data helped to distinguish non-cellular dependent processes from those resulting from reabsorption, secretion or release by cells. Extracellular metabolome profiling showed that some metabolites were more abundant after 6 h (e.g., lactic acid, ornithine; Fig. 4a) and 24 h (e.g., lactic acid, ornithine; Fig. 4b) of hypoxia, compared to their respective normoxic control. Others were decreased after 6-h (e.g., hexoses, uridine monophosphate; Fig. 4a) and 24-h hypoxia (e.g., hypoxanthine, D-ribose; Fig. 4b). Metabolites that increased or decreased in the supernatant upon reoxygenation (2, 24 and 48 h) following 6- or 24-h hypoxia relative to their respective controls are summarized in Table 1 – Part 2. Some metabolites were found in higher levels after 24 h than 6 h of hypoxia (lysine, niacinamide, pyridoxine, choline, proline) and others in lower levels (adenosine, hexoses, uridine monophosphate, cytidine, hypoxanthine, putrescine). Upon reoxygenation after 24-h hypoxia, none of the metabolites were found in higher or lower quantities in the extracellular medium as compared to equivalent reoxygenation duration after 6-h hypoxia.

Posterior predictive distribution of metabolites in conditions of (**a**) 6-h and (**b**) 24-h hypoxia without reoxygenation, in the extracellular environment. The points are the means, the thick and thin segments respectively the 80% and 98% confidence intervals of the posterior distribution. The green line (mean) and rectangles (80% and 98% credible intervals) are the posterior predictive distribution irrespective of metabolite. Metabolites are in red (over abundant) or blue (under abundant) if their 98% confidence intervals do not cross the 98% confidence interval for all the metabolites.

4 Discussion

We conducted an exploratory study to determine the effect of oxygen deprivation on the transport system in a human proximal tubular cell line. Some transporters showed transcriptional down- or up-regulation during prolonged hypoxia, but the metabolome rapidly returned

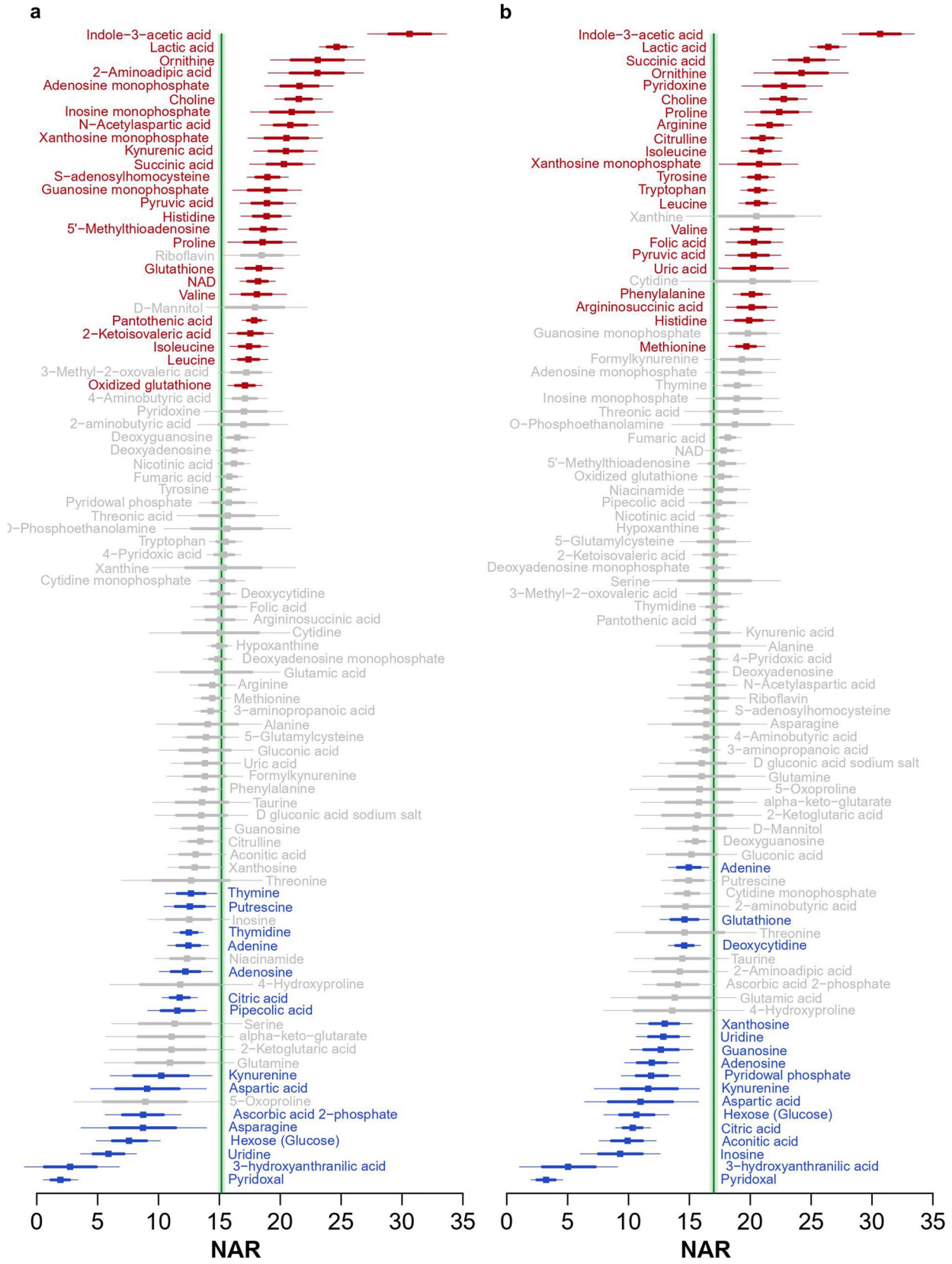

Fig. 3 Intracellular metabolomic profiling under hypoxia conditions

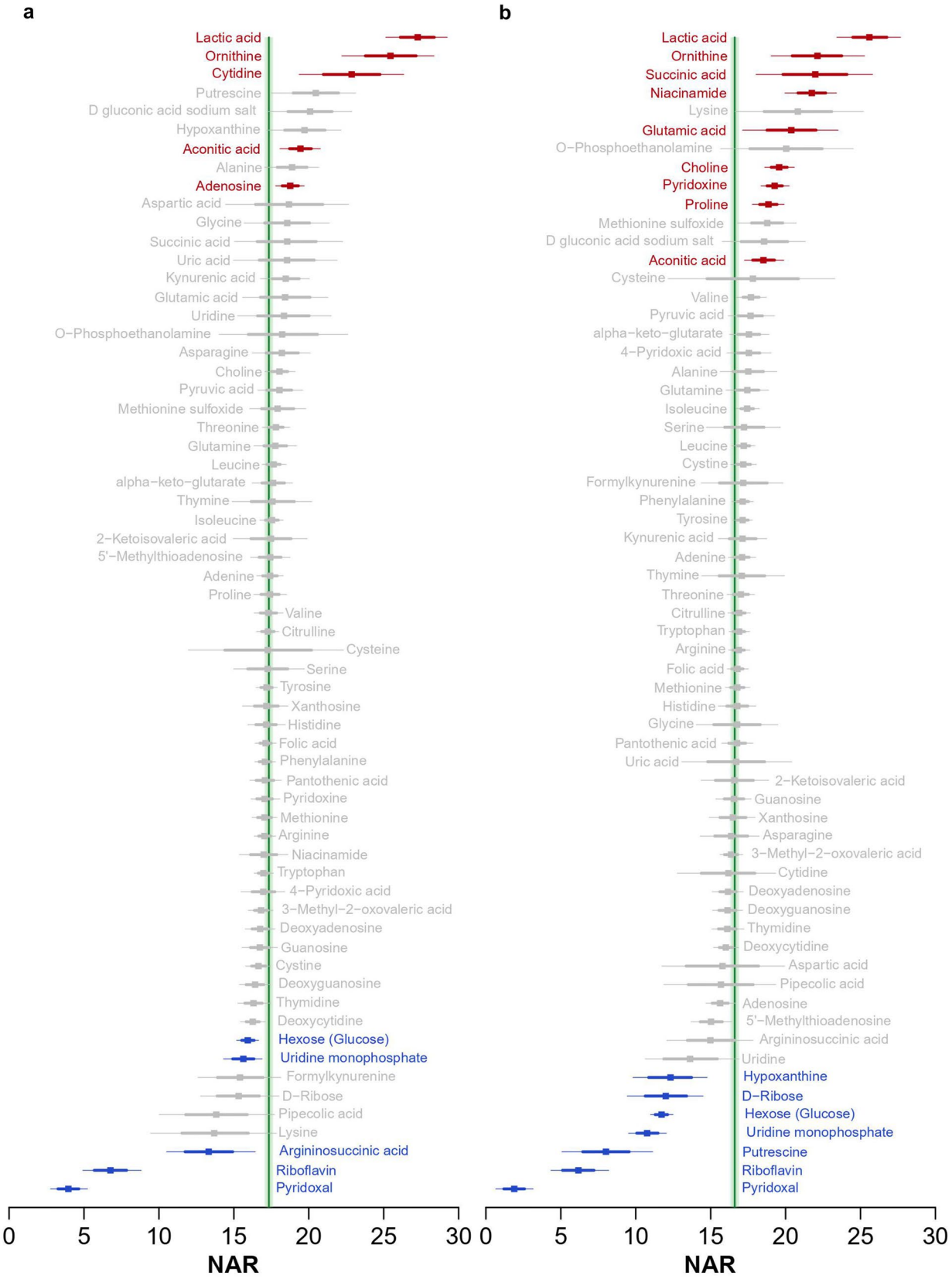

Fig. 4 Extracellular metabolomic profiling under hypoxia conditions

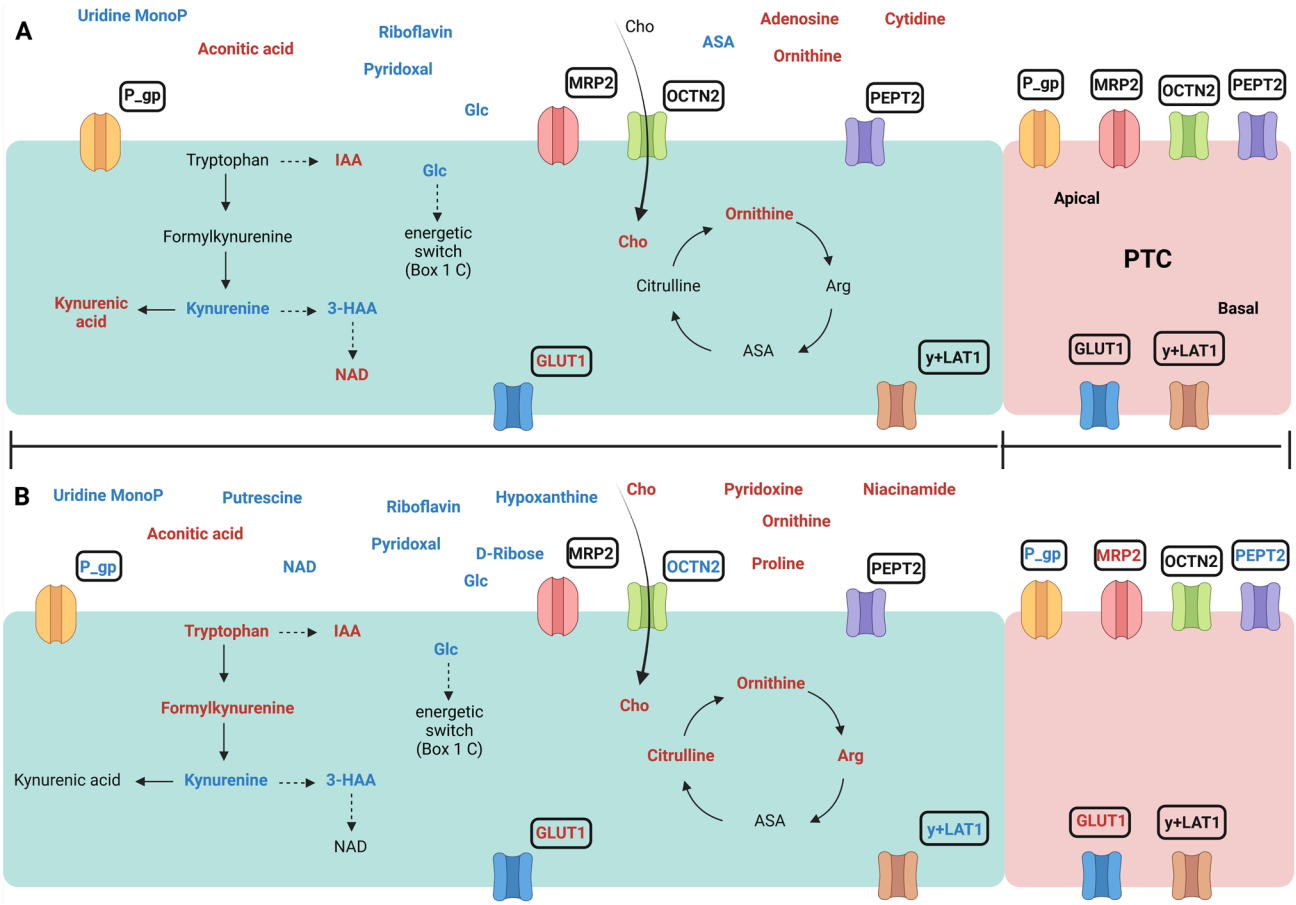

Fig. 5 Impact of hypoxia on metabolomics profiles and of hypoxia/reoxygenation on the mRNA expression or tubular transporters

Table 1 Metabolomic profiling in a human proximal tubular cell line in hypoxia/reoxygenation conditions

Part 1: Intracellular environment						
H (hours)	6			24		
R (hours)	2	24	48	2	24	48
Metabolites	**Lactic acid** *Phenylalanine* *Uridine* *Putrescine* *Hexoses*	**ASA** *Adenine* *Putrescine*	**ASA** *Adenine* *Putrescine*	**Lactic acid** **Pyridoxal** *Desoxycytidine* *Citric acid* *Putrescine*	**ASA** **Lactic acid** *Adenine* *Adenosine* *Xanthosine* *Guanosine*	**ASA** **Lactic acid** **Hypoxanthine** *Adenine* *Adenosine*
Part 2: Extracellular environment						
H (hours)	6			24		
R (hours)	2	24	48	2	24	48
Metabolites	**Lactic acid** **Pyruvic acid** *Hexoses* *Uridine*	**Lactic acid** **Pyruvic acid** **Pyridoxine** *Uridine* *Desoxycytidine* *Hexoses*	**Lactic acid** **Pyruvic acid** **Pyridoxine** *Hexoses* *Uridine*	**Lactic acid** **Pyruvic acid** **Pyridoxal** *Uridine*	**Lactic acid** **Pyruvic acid** **Pyridoxine** *Hexoses*	**Lactic acid** **Pyruvic acid** **Pyridoxine** **Proline** **Choline** *Hexoses*

Metabolites in bold characters are increased those in italics are decreased; variations are expressed according to their respective normoxic control; ASA, arginosuccinic acid; H, hypoxia; R, reoxygenation

to equilibrium upon cell reoxygenation and only weak disruption of exchanges between the cell and its environment was noted. These results suggest that in our conditions, the impact hypoxia and reoxygenation have on the expression of transporters does not significantly translate in cellular metabolome modifications (Fig. 5).

Overview of metabolomic and transporter perturbations in H-incubated PTC during (**a**) 6 h or (**b**) 24 h. PTC in blue represents hypoxia and in red the first two hours of reoxygenation. For reoxygenation, we have only represented expression variations of transporters. The metabolites and transporters in red increase, in blue decrease, and in black are unchanged compared to normoxia. 3-AA, 3-hydroxyanthranylic acid; IAA, indole-3-acetic acid; Arg, arginine; ASA, arginosuccinic acid; Cho, choline; Glc, glucose; MonoP, monophosphate; NAD, nicotinamide adenine dinucleotide. Illustration created with BioRender.com.

4.1 Hypoxia conditions lead to adaption of PTC

Albeit the impact of IR or ischemia on the expression of tubular transporters had already been documented using pre-clinical models, few studies have been conducted on hypoxia/reoxygenation kinetics using human cell lines. We opted for two hypoxia durations (6 h for brief and 24 h for prolonged hypoxia) and oxygen deprivation only (with glucose supplementation), according to our previous clinical study (Faucher et al. 2022), where cold ischemia duration was on average 1020 min (from 13 to 20 h) and glucose concentration in graft preservation fluids did not change with ischemia duration. Regarding reoxygenation effects, we focused on the early post-reperfusion period by studying variations after 2, 24 and 48 h. The effect of reoxygenation might extend beyond 48 h in transplanted patients, but to the best of our knowledge there is no clear indication about this. Overall, our results are thus indicative of changes that may occur in the pre- and early post-implantation period in the clinics, even though they are unlikely to replicate them exactly. We found here that hypoxia did not induce uncontrolled death of PTCs, and that these cells appeared to be more sensitive to prolonged hypoxia upon reoxygenation (Figure S3). We identified variations of some anaerobic glycolysis and TCA cycle intermediates, characteristic of ischemia (Fig.1), and of the glutathione metabolism pathway and ATP breakdown (Fig. 3a and S5a).

4.2 Expression of membrane transporters

We hypothesized that hypoxia duration affects the expression of tubular transporters and its recovery under reoxygenation. To this end, we evaluated the transcriptional expression of a large number of transporters expressed by human PTC. We selected transporters according to previous studies on pre-clinical models (Matsuzaki et al. 2007 & Schneider et al. 2011) and clinical data (Kwon et al. 2007), representing different tubular transport systems for energy metabolites (amino acids, glucose), and belonging to the SLC and ABC superfamilies involved in metabolite transport. Some of them are also the targets of clinically significant drug-drug interactions (Yin & Wang 2016).

Our transcriptomic study presents some limitations, including a lack of robustness highlighted by variations observed with different MRP4 primers, alternate and/or isolated up- and down-regulation of transporters (AQP3, NBCe1 (*slc4a4*), NaPiIIc (*slc34a3*), OCT1 (*slc22a1*), rBAT (*slc3a1*), MRP1 (*abcc1)* and SGLT2 (*slc5a2*))), and the high variability observed in normoxic conditions over time (Figure S4). For this reason, we will only discuss the most robust variations observed. More importantly, the transcripts encoding several tubular transporters were not detected in our conditions. Among them, OAT1/OAT2/OAT3 and GLUT2 were previously reported as absent (Secker et al. 2019), whereas OCT2, MATE1, MATE2, and BCRP were identified in this cell model (Secker et al. 2019 & Aschauer et al. 2015). Unfortunately, the absence of OAT1/3, OCT2, and MATE1 hampered the validation of previous observations in animal models. Indeed, a study showed decreased rOAT1 and rOAT3 protein expression at 48-h reperfusion after 30 min of warm ischemia in rats (Matsuzaki et al. 2007), whereas decreased rOCT1 and rOCT2 mRNA and protein expression was identified at 24-h reoxygenation after 45-min of warm ischemia (Schneider et al. 2011).

We observed downregulated aquaporins (AQP1 and AQP2) only after 24-h hypoxia, persisting during reoxygenation. For AQP2, the upregulation observed after 24- and 48-h reoxygenation after 6-h hypoxia suggests a secondary compensation mechanism. This downregulation of AQP1 and AQP2 during hypoxia might be explained by the necessity for PTC to limit water uptake and prevent cellular edema.

Many studies mostly reported downregulations of SLCs during ischemia (Faucher et al. 2020 & Barin-Le Guellec et al. 2018). Our results showed a similar tendency, except for GLUT1 (*slc2a1*). We observed that some transporters were not affected by hypoxia or reoxygenation, especially those of the amino acid transport system (e.g. EAAT3 (*slc1a1*) 4F2hc (*slc3a2*), LAT2 (*slc7a8*)) and NaDC3 (*slc13a3*); Fig. 2a). Differential hypoxia-dependent modifications of ABC transporters (up-regulation for MRP2 and down-regulation for P-gp after 2-h reoxygenation) were observed. Interestingly, the expression profile of some transporters was modified during hypoxia (y^+LAT1 (*slc7a7*) and OCTN2 (*slc22a5*)), reoxygenation (MRP2 (*abcc2*),

PEPT1/2 (*slc15a1/2*), OATP4C1 (*slco4c1*)) or both (P-gp (*abcb1*) and GLUT1 (*slc2a1*)), suggesting that the effects of the yet unclear underlying molecular mechanisms can be sustained or appear during early reoxygenation, and are sensitive to hypoxia duration. We did not observe any significant transcript variation at 48-h reoxygenation after 6- or 24-h hypoxia (except for OATP4C1), showing the transient nature of transporter expression perturbations. However, the recovery of gene expression during reoxygenation does not necessarily imply the absence of protein variations, since the kinetics of transcription and protein expression generally differ (Faucher et al. 2020).

4.3 Evolution of extra/intra-cellular endogenous metabolome under hypoxia and reoxygenation

As mentioned above, IRI induces ischemia-dependent metabolic disturbances and a post-reperfusion metabolic collapse (Lindeman et al. 2020). We used semi-targeted profiling of the endogenous metabolome to determine its evolution under hypoxia and reoxygenation conditions, to try and decipher the underlying mechanisms of IRI. We conducted independent analyses of the extracellular and intracellular metabolome to discriminate secreted and absorbed metabolites and find possible endogenous metabolite/transporter relationships.

We assessed the time-dependent intracellular metabolic changes under hypoxia/reoxygenation. In addition to the well-known perturbation of the energetic pathway, we found alterations in the kynurenine pathway which is sensitive to the redox balance (González Esquivel et al. 2017). The decrease in kynurenine and 3-HAA was observed after 6- and 24-h hypoxia. The increase of kynurenic acid during brief hypoxia, of tryptophan and formylkynurenine after 24 h, and of indole-3-acetic acid after 6 and 24 h suggest a progressive requirement from the kynurenine-(3-HAA) pathway to maintain NAD coenzyme levels, since the impairment of*de novo*NAD biosynthesis is an aggravating risk factor for AKI (Poyan Mehr et al. 2018). Metabolome stabilization was observed promptly after cellular reoxygenation. It is worth mentioning that metabolome variations were highly time-dependent and did not necessarily reflect the underlying (pathway or transport) disorders. Additional fluxomic approaches could provide further information on the metabolic flux perturbations occurring under reoxygenation (Cortassa et al. 2015). However, this rapid equilibrium shows that hypoxia at 37 °C did not induce a large-scale metabolic perturbation of PTC upon reoxygenation, indirectly supporting the use of normothermic machine perfusion in transplantation (Elliott et al. 2021). However, the absence of data obtained in a hypothermic environment hampers direct comparisons between these two conditions in our study.

Analyzing the extracellular metabolome was meant to understand the IR-associated mechanisms and identify metabolites potentially reflecting transport activities. The absence of cytotoxicity with H/R implies that the extracellular metabolic changes are independent from cell lysis. The decrease in extracellular glucose under hypoxia and up to 48-h reoxygenation and the secretion of lactic and pyruvic acid over the same time period confirm the energetic switch. We observed a higher amount of choline only after 24 h of hypoxia, which could be related to its lower reabsorption during prolonged hypoxia. Increased ornithine concentration reflects the cellular stimulation of the urea cycle. Only few variations were found in the exchanges between the cell and its extracellular environment upon reoxygenation, suggesting rapid adaptation of cellular pathways and transport activities to maintain homeostasis.

4.3.1 Transcriptional expression of membrane transporters and metabolomic variations

In this study, we investigate the interdependence between the intra/extracellular metabolomic profiles and the mRNA expression of transporters, as proposed in our clinical study report (Faucher et al. 2022). We found an increase in transcriptional GLUT1 expression under hypoxia (6 and 24 h). However, GLUT1 is involved in glucose transport from the intracellular to the extracellular space at the basolateral pole of PTC. Its overexpression is inconsistent with increased intracellular glucose.

Kynurenic acid is excreted by MRP4 and BCRP (Dankers et al. 2013). Its transient increase in the intracellular compartment and the absence of variation of its extracellular concentration suggests a modulation of its transporter-dependent excretion under hypoxia. However, we have not identified the mRNA coding for BCRP and the variations observed for MRP4 remain uncertain. On the other hand, we observed a decrease in choline reabsorption only after 24-h hypoxia. This is consistent with the tendency to OCTN2 downregulation after 24-h hypoxia since choline is reabsorbed at the apical membrane by OCTN2 (Koepsell et al. 2007). However, intracellular choline remained elevated in hypoxia, suggesting other compensatory mechanisms. Overall, we did not find clear transporter-related metabolic variations. This can be explained by: (i) the consumption or production of endogenous transporters' substrates; (ii) a shift between transcriptomic and protein expression; and/or (iii) inter-transporter compensatory transport mechanisms favoring metabolic homeostasis. This highlights the limitation of isolated systems to study cellular metabolic and transport functions together. Moreover, the expression of some transporters can directly influence the cellular production of endogenous metabolites since OAT1 and OAT3 expression affects cellular

energy metabolism and the synthesis of α-ketoglutarate (Vriend et al. 2019). Further studies of the hypoxia-sensitive transporters identified here must now be undertaken. Finally, the use of a broader spectrum metabolomics-based method could enlarge the scope of potential transporter substrates.

The influence of ischemia on tubular transporters expression during kidney conservation has not been extensively studied in humans. Kown et al. reported a misdistribution of hOAT1 on post-ischemic biopsies obtained 1 h after reperfusion during transplant operation (Kwon et al. 2007). In contrast, we previously reported that the transcriptomic expression of the transporters was not different according to graft preservation duration on a perfusion machine in a cohort of transplant patients (Faucher et al. 2022). The transporter perturbations observed in pre-clinical models during reperfusion may be more related to protein impairment or malfunction and to perturbations of the handling of "systemic" substrates, than to transcriptomic expression. The limited ability to study transporters in 2D cell models is the major limitation of this work (Fransen et al. 2021 & Wilmer et al. 2016). A microphysiological system based on a bi-compartmentation and microfluidic environment will be considered to study tubular transports further (Wilmer et al. 2016 & Jansen et al. 2016). IR-mimicking micro-perfusion systems have recently been proposed (Giraud et al. 2020 & Zamorano et al. 2021). These studies should also investigate the possible interaction between uremic toxins, drugs and endogenous metabolites to shed light on the impact of tubular transporter disruption on the recovery of renal transplant function. Isotope-labeled exogenous substrates may permit to unravel the influence of transporters on substrate transport and the underlying metabolic pathways (Nath et al. 2016). Further studying the ischemia-dependent modulations of transporters is important, notably to prevent the administration of drugs which are substrates of these transporters, or potentially to facilitate their restoration using targeted inducers (Faucher et al. 2020). Moreover, in the context of pre-implantation graft preservation on perfusion machines, the disruption of transporter functions could impact the therapeutic efficacy of exogenous molecules used as pre-transplant therapies (Hosgood et al. 2021).

5 Conclusion

We have studied the impact of hypoxia and reoxygenation on the transcriptional expression of a large number of SLC and ABC transporters constituting the membrane transport systems of human proximal tubular cells. This study shows dysregulations of the transcriptional expression of transporters in PTC during oxygen deprivation. The underlying molecular mechanisms are unclear, but their effects on transporters can be sustained or appear during early reoxygenation, and are sensitive to hypoxia duration. Cellular reoxygenation was accompanied by a rapid return to metabolic equilibrium. We did not find any relationship between perturbations among a large set of endogenous metabolites and transporters' expression. This highlights the limitation of isolated systems to study cells' metabolic and transport functions together. Studying the tubular transport system of, and metabolic disturbances in, the proximal tubule is challenging due to the large numbers of transporters and substrates involved, and to the multispecific nature of numerous substrates. Given this complexity, we call for further studies targeting preselected transcellular transports using specific substrates to better investigate the connection between membrane transport and metabolic disturbances.

Supplementary Information The online version contains supplementary material available at https://doi.org/10.1007/s11306-023-02044-4.

Acknowledgements The authors thank the Nouvelle Aquitaine Region and INSERM for their financial support, and BISCEm US042 INSERM—UMS 2015 CNRS, Molecular Analysis Platform for technical support. The authors are grateful to Karen Poole for correcting English, and Jean-Sebastien Bernard and Marie Piollet for helping with the experiments.

Author contributions QF: Conceived and designed study, performed research, analyzed data, writing (original draft, reviewing & editing). SC: Conceived and designed study, analyzed data, writing (reviewing & editing). AH: Analyzed data, writing (reviewing & editing). FLS: Performed research, analyzed data, writing (reviewing & editing). HA: Performed research, analyzed data, writing (reviewing & editing). PG: Conceived and designed study, writing (reviewing & editing). MB: Conceived and designed study, writing (reviewing & editing). SR: Conceived and designed study, writing (reviewing & editing). RL: Conceived and designed study, writing (reviewing & editing). PM: Conceived and designed study, writing (reviewing & editing). CBLG: Conceived and designed study, writing (reviewing & editing).

Funding This work was supported by Région Nouvelle Aquitaine and « Institut National de la Santé et de la Recherche Médicale » (INSERM).

Data availability Detailed statistical analyses for metabolomic data, as well as the scripts used are available in https://inserm_pharmacology_limoges.gitlab.io/2023_faucher_sd_statistics_metabolomics/. Data and data set generated during the current study are available from the corresponding author on reasonable request.

Declarations

Conflict of interest The authors have no competing interests to disclose.

References

Aschauer, L., Gruber, L. N., Pfaller, W., et al. (2013). Delineation of the key aspects in the regulation of epithelial monolayer formation. *Molecular and Cellular Biology*, *33*, 2535–2550. https://doi.org/10.1128/MCB.01435-12.

Aschauer, L., Carta, G., Vogelsang, N., et al. (2015). Expression of xenobiotic transporters in the human renal proximal tubule cell line RPTEC/TERT1. *Toxicology in Vitro*, *30*, 95–105. https://doi.org/10.1016/j.tiv.2014.12.003.

Barin-Le Guellec, C., Largeau, B., Bon, D., et al. (2018). Ischemia/reperfusion-associated tubular cells injury in renal transplantation: Can metabolomics inform about mechanisms and help identify new therapeutic targets? *Pharmacological Research*, *129*, 34–43. https://doi.org/10.1016/j.phrs.2017.12.032.

Chen, C. C., Chapman, W. C., & Hanto, D. W. (2015). Ischemia-reperfusion injury in kidney transplantation. *Frontiers in Bioscience (Elite Ed), 7*, 117–134.

Cortassa, S., Caceres, V., Bell, L. N., et al. (2015). From metabolomics to fluxomics: A computational procedure to translate metabolite profiles into metabolic fluxes. *Biophys J, 108*, 163–172. https://doi.org/10.1016/j.bpj.2014.11.1857

Dankers, A. C. A., Mutsaers, H. A. M., Dijkman, H. B. P. M., et al. (2013). Hyperuricemia influences tryptophan metabolism via inhibition of multidrug resistance protein 4 (MRP4) and breast cancer resistance protein (BCRP). *Biophysica Acta (BBA) - Molecular Basis of Disease, 1832*, 1715–1722. https://doi.org/10.1016/j.bbadis.2013.05.002

Elliott, T. R., Nicholson, M. L., & Hosgood, S. A. (2021). Normothermic kidney perfusion: An overview of protocols and strategies. *American Journal of Transplantation*, *21*, 1382–1390. https://doi.org/10.1111/ajt.16307.

Faucher, Q., Alarcan, H., Marquet, P., & Barin-Le Guellec, C. (2020). Effects of ischemia-reperfusion on tubular cell membrane transporters and consequences in kidney transplantation. *Journal of Clinical Medicine*. https://doi.org/10.3390/jcm9082610

Faucher, Q., Alarcan, H., & Sauvage, F. L. (2022). Perfusate metabolomics content and expression of tubular transporters during human kidney graft preservation by hypothermic machine perfusion. *Transplantation*. https://doi.org/10.1097/TP.0000000000004129

Fransen, M. F. J., Addario, G., Bouten, C. V. C., et al. (2021). Bioprinting of kidney in vitro models: cells, biomaterials, and manufacturing techniques. *Essays in Biochemistry*. https://doi.org/10.1042/EBC20200158

Giraud, S., Thuillier, R., Cau, J., & Hauet, T. (2020). In vitro/ex vivo models for the study of ischemia reperfusion injury during kidney perfusion. *International Journal of Molecular Sciences, 21*, 8156. https://doi.org/10.3390/ijms21218156

González Esquivel, D., Ramírez-Ortega, D., Pineda, B., et al. (2017). Kynurenine pathway metabolites and enzymes involved in redox reactions. *Neuropharmacology*, *112*, 331–345. https://doi.org/10.1016/j.neuropharm.2016.03.013.

Hosgood, S. A., Hoff, M., & Nicholson, M. L. (2021). Treatment of transplant kidneys during machine perfusion. *Transplant International*, *34*, 224–232. https://doi.org/10.1111/tri.13751.

Jouret, F., Leenders, J., Poma, L., et al. (2016). Nuclear magnetic resonance metabolomic profiling of mouse kidney, urine and serum following renal ischemia/reperfusion Injury. *Plos One, 11*, e0163021. https://doi.org/10.1371/journal.pone.0163021

Koepsell, H., Lips, K., & Volk, C. (2007). Polyspecific organic cation transporters: Structure, function, physiological roles, and biopharmaceutical implications. *Pharmaceutical Research*, *24*, 1227–1251. https://doi.org/10.1007/s11095-007-9254-z.

Kwon, O., Hong, S. M., & Blouch, K. (2007). Alteration in renal organic anion transporter 1 after ischemia/reperfusion in cadaveric renal allografts. *Journal of Histochemistry and Cytochemistry*, *55*, 575–584. https://doi.org/10.1369/jhc.6A7130.2007.

Jansen, J., Fedecostante, M., Wilmer, M. J., et al. (2016). Bioengineered kidney tubules efficiently excrete uremic toxins. *Scientific Reports*, *6*, 26715. https://doi.org/10.1038/srep26715.

Lindeman, J. H., Wijermars, L. G., Kostidis, S., et al. (2020). Results of an explorative clinical evaluation suggest immediate and persistent post-reperfusion metabolic paralysis drives kidney ischemia reperfusion injury. *Kidney International*, *98*, 1476–1488. https://doi.org/10.1016/j.kint.2020.07.026.

Malagrino, P. A., Venturini, G., Yogi, P. S., et al. (2016). Metabolomic characterization of renal ischemia and reperfusion in a swine model. *Life Sciences*, *156*, 57–67. https://doi.org/10.1016/j.lfs.2016.05.025.

Matsuzaki, T., Watanabe, H., Yoshitome, K., et al. (2007). Downregulation of organic anion transporters in rat kidney under ischemia/reperfusion-induced acute [corrected] renal failure. *Kidney International*, *71*, 539–547. https://doi.org/10.1038/sj.ki.5002104.

Nath, J., Smith, T., Hollis, A., et al. (2016). 13C glucose labelling studies using 2D NMR are a useful tool for determining ex vivo whole organ metabolism during hypothermic machine perfusion of kidneys. *Transplant Research, 5*, 7. https://doi.org/10.1186/s13737-016-0037-0

Nath, J., Smith, T. B., Patel, K., et al. (2017). Metabolic differences between cold stored and machine perfused porcine kidneys: A 1H NMR based study. *Cryobiology*, *74*, 115–120. https://doi.org/10.1016/j.cryobiol.2016.11.006.

Nieuwenhuijs-Moeke, G. J., Pischke, S. E., Berger, S. P., et al. (2020). Ischemia and reperfusion injury in kidney transplantation: Relevant mechanisms in injury and repair. *Journal of Clinical Medicine, 9*, 253. https://doi.org/10.3390/jcm9010253

Poyan Mehr, A., Tran, M. T., Ralto, K. M., et al. (2018). De novo NAD + biosynthetic impairment in acute kidney injury in humans. *Nature Medicine*, *24*, 1351–1359. https://doi.org/10.1038/s41591-018-0138-z.

Schneider, R., Meusel, M., Betz, B., et al. (2011). Nitric oxide-induced regulation of renal organic cation transport after renal ischemia-reperfusion injury. *American Journal of Physiology. Renal Physiology, 301*, F997–F1004. https://doi.org/10.1152/ajprenal.00264.2011

Secker, P. F., Schlichenmaier, N., Beilmann, M., et al. (2019). Functional transepithelial transport measurements to detect nephrotoxicity in vitro using the RPTEC/TERT1 cell line. *Archives of Toxicology*, *93*, 1965–1978. https://doi.org/10.1007/s00204-019-02469-8.

Stryjak, I., Warmuzińska, N., Bogusiewicz, J., et al. (2020). Monitoring of the influence of long-term oxidative stress and ischemia on the condition of kidney using solid phase microextraction chemical biopsy coupled with liquid chromatography high resolution mass spectrometry. *Journal of Separation Science*. https://doi.org/10.1002/jssc.202000032.

Wang, Z., Lyu, Z., Pan, L., et al. (2019). Defining housekeeping genes suitable for RNA-seq analysis of the human allograft kidney biopsy tissue. *BMC Medical Genomics, 12*, 86. https://doi.org/10.1186/s12920-019-0538-z

WHO (May 2021). Projections of mortality and causes of death, 2016 to 2060. In: WHO. http://www.who.int/healthinfo/global_burden_disease/projections/en/. Accessed 22 .

Vriend, J., Hoogstraten, C. A., Venrooij, K. R., et al. (2019). Organic anion transporters 1 and 3 influence cellular energy metabolism in renal proximal tubule cells. *Biological Chemistry*, *400*, 1347–1358. https://doi.org/10.1515/hsz-2018-0446.

Wilmer, M. J., Ng, C. P., Lanz, H. L., et al. (2016). Kidney-on-a-chip technology for drug-induced nephrotoxicity screening. *Trends in*

Biotechnology, 34, 156–170. https://doi.org/10.1016/j.tibtech.2015.11.001

Wong, G., Teixeira-Pinto, A., Chapman, J. R., et al. (2017). The impact of total ischemic time, donor age and the pathway of donor death on graft outcomes after deceased donor kidney transplantation. *Transplantation, 101*, 1152–1158. https://doi.org/10.1097/TP.0000000000001351

Yin, J., & Wang, J. (2016). Renal drug transporters and their significance in drug–drug interactions. *Acta Pharmaceutica Sinica B*, *6*, 363. https://doi.org/10.1016/j.apsb.2016.07.013.

Yuan, M., Breitkopf, S. B., Yang, X., & Asara, J. M. (2012). A positive/negative ion-switching, targeted mass spectrometry-based metabolomics platform for bodily fluids, cells, and fresh and fixed tissue. *Nature Protocols*, *7*, 872–881. https://doi.org/10.1038/nprot.2012.024.

Zamorano, M., Castillo, R. L., Beltran, J. F., et al. (2021). Tackling ischemic reperfusion injury with the aid of stem cells and tissue engineering. *Frontiers in Physiology, 12*, 1436. https://doi.org/10.3389/fphys.2021.705256

Zhao, H., Alam, A., Soo, A. P., et al. (2018). Ischemia-reperfusion injury reduces long term renal graft survival: Mechanism and beyond. *EBioMedicine, 28*, 31–42. https://doi.org/10.1016/j.ebiom.2018.01.025